STRUCTURAL BIOLOGY
COMMUNICATIONS

ISSN: 2053-230X
journals.iucr.org/f

Overexpression, purification and crystallization of the response regulator NsrR involved in nisin resistance

Sakshi Khosa, Astrid Hoeppner, Diana Kleinschrodt and Sander H. J. Smits

Acta Cryst. (2015). F**71**, 1322–1326

STRUCTURAL BIOLOGY COMMUNICATIONS

ISSN 2053-230X

Overexpression, purification and crystallization of the response regulator NsrR involved in nisin resistance

Sakshi Khosa,[a] Astrid Hoeppner,[b] Diana Kleinschrodt[c] and Sander H. J. Smits[a]*

[a]Institute of Biochemistry, Heinrich-Heine-University, Universitätsstrasse 1, 40225 Düsseldorf, Germany, [b]Crystal Farm and X-ray Facility, Heinrich-Heine-University, Universitätsstrasse 1, 40225 Düsseldorf, Germany, and [c]Protein Production Facility, Heinrich-Heine-University, Universitätsstrasse 1, 40225 Düsseldorf, Germany. *Correspondence e-mail: sander.smits@hhu.de

Received 4 August 2015
Accepted 3 September 2015

Edited by R. L. Stanfield, The Scripps Research Institute, USA

Keywords: response regulator; nisin; lantibiotic; resistance; X-ray analysis.

Supporting information: this article has supporting information at journals.iucr.org/f

A number of Gram-positive bacteria produce a class of bacteriocins called 'lantibiotics'. These lantibiotics are ribosomally synthesized peptides that possess high antimicrobial activity against Gram-positive bacteria, including clinically challenging pathogens, and are therefore potential alternatives to antibiotics. All lantibiotic producer strains and some Gram-positive non-producer strains express protein systems to circumvent a suicidal effect or to become resistant, respectively. Two-component systems consisting of a response regulator and a histidine kinase upregulate the expression of these proteins. One of the best-characterized lantibiotics is nisin, which is produced by *Lactococcus lactis* and possesses bactericidal activity against various Gram-positive bacteria, including some human pathogenic strains. Within many human pathogenic bacterial strains inherently resistant to nisin, a response regulator, NsrR, has been identified which regulates the expression of proteins involved in nisin resistance. In the present study, an expression and purification protocol was established for the NsrR protein from *Streptococcus agalactiae* COH1. The protein was successfully crystallized using the vapour-diffusion method, resulting in crystals that diffracted X-rays to 1.4 Å resolution.

1. Introduction

The increasing incidence of antibiotic resistance has led to an urgent need for alternative therapeutic options. A potential class of alternatives are small ribosomally synthesized antimicrobial peptides called lantibiotics, which are produced by various Gram-positive bacteria. Lantibiotics bind to lipid II, an essential cell-membrane precursor, forming a complex that inhibits cell-wall synthesis and forms pores within the membrane (Breukink & de Kruijff, 2006; Hsu *et al.*, 2004). Lantibiotics have a wide antibacterial efficacy and their therapeutic potential has already been recognized (Hancock & Sahl, 2006; Boakes & Wadman, 2008).

The best-characterized lantibiotic is nisin, which is produced by some *Lactococcus lactis* strains and has a wide bactericidal activity spectrum against human pathogenic strains including *Clostridium difficile* and methicillin-resistant *Staphylococcus aureus* (MRSA) (Bartoloni *et al.*, 2004; Severina *et al.*, 1998; Cotter *et al.*, 2005). Nisin has also been used in the food industry as a food preservative (Delves-Broughton *et al.*, 1996).

All nisin producer strains naturally express an immunity system to avoid a suicidal effect. However, there are also some nisin-nonproducing strains, including various pathogenic bacteria such as *Streptococcus agalactiae* and *S. aureus*, which are naturally resistant to nisin (Harris *et al.*, 1992). There is a

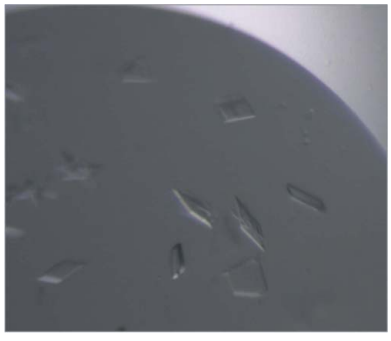

Table 1
Macromolecule-production information.

Source organism	*S. agalactiae*
DNA source	*S. agalactiae*
Forward primer	GGAGGGCATATGTCACAAGAGCAAGG
Reverse primer	GGAATCGGATCCTGTAGTAAATACCCAACTCC
Expression vector	pET-24a
Expression host	*E. coli* BL21 (DE3)
Complete amino-acid sequence of the construct produced	MSQEQGKIYIVEDDMTIVSLLKDHLSASYHVSSV-SNFRDVKQEIIAFQPDLILMDITLPYFNGFYW-TAELRKFLTIPIIFISSSNDEMDMVMALNMGG-DDFISKPFSLAVLDAKLTAILRRSQQFIQQEL-TFGGFTLTREGLLSSQDKEVILSPTENKILSI-LLMHPKQVVSKESLLEKLWENDSFIDQNTLNV-NMTRLRKKIVPIGFDYIHTVRGVGYLLQDPNS-SSVDKLAAALEHHHHHH

whole gene operon associated with the mechanism of nisin resistance, which was recently found in various species of Gram-positive human-pathogenic bacteria. The operon consists of four genes which encode the nisin-resistance protein NSR, a two-component system (TCS) and an ABC transporter (Khosa *et al.*, 2013).

The TCS comprises a sensor histidine kinase (NsrK) localized in the membrane and a response regulator (NsrR). NsrK is autophosphorylated upon external signal (in this case, nisin) and the phosphate is then transferred to an aspartate residue of the response regulator NsrR. This phosphorylation activates the regulator, thereby triggering transcription of the genes (Stock *et al.*, 2000; Khosa *et al.*, 2013).

Various two-component systems have been identified which are involved in lantibiotic resistance (Draper *et al.*, 2015; Kawada-Matsuo, Oogai *et al.*, 2013). The BraRS, GraRS and VraSR TCSs of *S. aureus* are associated with resistance against bacitracin, nisin and nukacin ISK-1 (Kawada-Matsuo, Yoshida *et al.*, 2013). The LiaRS and CprRK TCSs were also shown to be involved in resistance against antimicrobial peptides in *Listeria monocytogenes* and *Clostridium difficile*, respectively (Bergholz *et al.*, 2013; Suárez *et al.*, 2013). The presence of these numerous TCS members emphasizes their importance in lantibiotic resistance. Thus, the structure of the response regulator involved would help to expand our restricted knowledge regarding the underlying mechanism of lantibiotic resistance involving response regulators.

In this study, we present the overexpression, purification and crystallization of the response regulator from *S. agalactiae*, NsrR.

2. Materials and methods

2.1. Macromolecule production

2.1.1. Cloning and expression. The GBSCOH1_0895 gene (accession No. HG939456.1) from *S. agalactiae* COH1 was amplified by PCR using chromosomal DNA as template and the primer pair NsrR-for (GGAGGGCATATGTCACAAGAGCAAGG) and NsrR-rev (GGAATCGGATCCTGTAGTAAATACCCAACTCC). The PCR fragment was digested with NdeI and BamHI and ligated into pET-24a, with a His_6 tag introduced at the C-terminus. The resulting plasmid pET-24a-NsrR (Table 1) was verified by sequencing and subsequently transformed into *Escherichia coli* BL21 (DE3) cells for expression. A single transformed colony was inoculated into 20 ml LB medium containing 30 µg ml^{-1} kanamycin. The culture was grown for 14 h at 310 K with shaking at 200 rev min^{-1}. 4 l LB medium with 30 µg ml^{-1} kanamycin was inoculated with the overnight culture at an OD_{600} of 0.05 and grown at 310 K with shaking at 170*g* until an OD_{600} of 0.3 was reached. The temperature was lowered to 291 K and the cells were further grown to an OD_{600} of 0.8 before induction with 1 m*M* IPTG. The cells were grown for a further 15 h. The cells were harvested by centrifugation at 8000 rev min^{-1} for 20 min at 277 K. The harvested cell pellet was stored at 253 K until further use.

2.1.2. Purification. In the purification of NsrR, all steps were performed at 277 K. The stored cell pellet was thawed and resuspended in 10 ml buffer *A* [50 m*M* Tris pH 8.0, 50 m*M* NaCl, 2 m*M* PMSF, 10%(*v*/*v*) glycerol] and 10 mg DNase (deoxyribonuclease I from bovine pancreas; Sigma–Aldrich) was added. The cells were lysed five times using a cell disruptor (Constant Cell Disruption Systems, UK) at 160 MPa. The lysate was centrifuged at 42 000 rev min^{-1} for 60 min using a Ti-60 rotor to remove unlysed cells and debris.

Imidazole was added to the cleared lysate to a final concentration of 20 m*M*. The lysate was then applied onto an Ni^{2+}-loaded HiTrap HP Chelating column (GE Healthcare) pre-equilibrated with buffer *B* (20 m*M* Tris pH 8.0, 250 m*M* NaCl, 20 m*M* imidazole) at a flow rate of 1 ml min^{-1}. The column was washed with six column volumes of buffer *B*. The protein was then eluted with increasing concentrations of imidazole from 20 to 400 m*M* in form of a linear gradient spanning 60 min with a flow rate of 2 ml min^{-1}. The fractions containing the protein of interest were pooled and concentrated to 8 mg ml^{-1} in an Amicon centrifugal filter concentrator with a 10 kDa cutoff membrane (Millipore). The concentrated protein was then further purified by size-exclusion chromatography using a Superdex 200 GL 10/300 column (GE Healthcare) equilibrated with buffer *C* (25 m*M* Tris pH 9.0, 50 m*M* NaCl, 2 m*M* PMSF). The protein eluted as a single homogeneous peak and the fractions containing the protein were pooled and concentrated to 11 mg ml^{-1} as mentioned before. The purity of the protein was analyzed with 15% SDS–PAGE and colloidal Coomassie stain (Dyballa & Metzger, 2009). The purified protein was directly used for crystallization. Macromolecule-production information is summarized in Table 1.

2.2. Crystallization

Crystallization screening was performed at 285 K using an NT8 robot (Formulatrix) and the sitting-drop vapour-diffusion method in Corning 3553 sitting-drop plates. For initial screening, various commercial crystallization screens were used [NeXtal JCSG Core Suites I, Classics Suite, PEGs Suite and MPD Suite (Qiagen, Germany) and MIDAS (Molecular Dimensions, England)]. Nanodrops consisting of 0.1 µl each of protein solution and reservoir solution were mixed and

Table 2
Crystallization.

Method	Vapour diffusion
Plate type	Sitting-drop vapour diffusion
Temperature (K)	285
Protein concentration (mg ml^{-1})	11
Buffer composition of protein solution	25 m*M* Tris pH 9.0, 50 m*M* NaCl, 2 m*M* PMSF
Composition of reservoir solution	PEG 1500 [21, 23, 25, 28 or 30%(*w*/*v*)] and buffer pH 6.0, 7.0, 8.0 or 9.0
Volume and ratio of drop	1 µl:1 µl
Volume of reservoir (µl)	500

equilibrated against 50 µl reservoir solution. The screening yielded initial rectangular plate-shaped crystals after 2 d in the condition 0.1 *M* SPG buffer (succinic acid:sodium dihydrogen phosphate:glycine in a molar ratio of 2:7:7) pH 8.0, 25%(*w*/*v*) PEG 1500 (PACT suite condition A5). The initial crystals were optimized by varying the concentration of PEG [21, 23, 25, 28 and 30%(*w*/*v*)] and the pH of the buffer (6.0, 7.0, 8.0 and 9.0) using the sitting-drop vapour-diffusion method at 285 K. Crystals of similar quality appeared throughout the conditions. Each drop consisted of 1 µl protein solution (at a concentration of 11 mg ml^{-1}) mixed with 1 µl reservoir solution and was equilibrated against a reservoir volume of 500 µl. Crystals were obtained after 1 d and grew to maximum dimensions of 80 × 40 × 20 µm within 3 d. Crystallization information is summarized in Table 2.

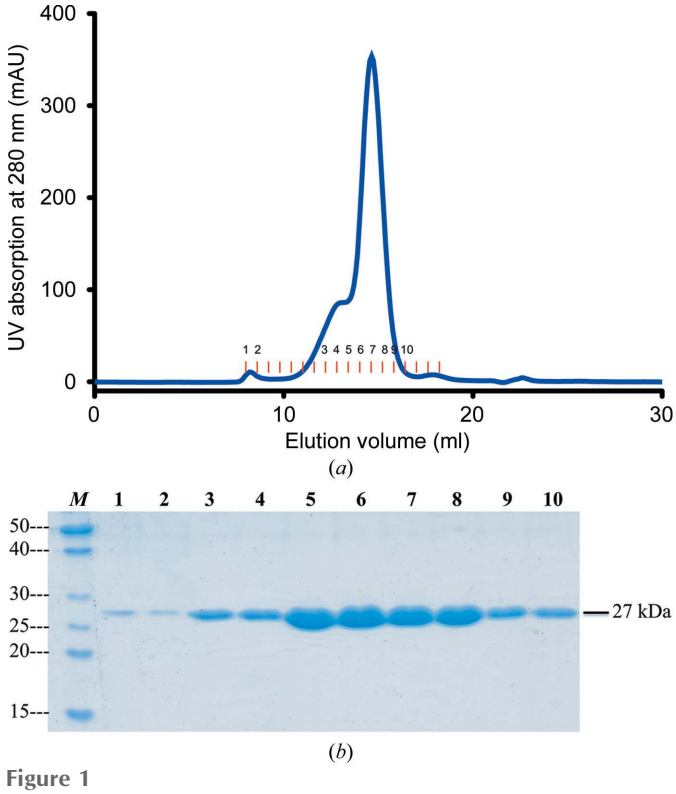

Figure 1
Purification of NsrR. (*a*) Chromatogram representing the purification of NsrR by size-exclusion chromatography. The *y* axis represents the UV absorption of the protein at 280 nm, while the *x* axis represents the elution volume. The red lines indicate the fractions collected. (*b*) 15% SDS–PAGE showing the purified NsrR fractions. Lane *M* contains molecular-mass marker (labelled in kDa); lanes 1–10 contain the corresponding purified NsrR fractions from the size-exclusion chromatogram displayed in (*a*).

Table 3
Data collection and processing.

Values in parentheses are for the outer shell.

Diffraction source	ID30A-3, ESRF
Wavelength (Å)	0.9677
Temperature (K)	100
Detector	Pilatus3 2M
Crystal-to-detector distance (mm)	148.66
Rotation range per image (°)	0.1
Total rotation range (°)	130
Exposure time per image (s)	0.02
Space group	$P2_12_12$ or $P2_12_12_1$
a, *b*, *c* (Å)	56.3, 60.4, 56.8
α, β, γ (°)	90, 90, 90
Mosaicity (°)	0.047
Resolution range (Å)	100.0–1.4 (1.45–1.40)
Total No. of reflections	183274 (18114)
No. of unique reflections	38706 (3801)
Completeness (%)	99.3 (98.6)
Multiplicity	4.7 (4.8)
$\langle I/\sigma(I)\rangle$	13.2 (1.7)
R_{meas}† (%)	6.3 (91.6)
Overall *B* factor from Wilson plot (Å^2)	24.6
Matthews coefficient V_M (Å^3 Da^{-1})	1.75
Solvent content (%)	29.6

† $R_{meas} = \sum_{hkl}\{N(hkl)/[N(hkl)-1]\}^{1/2}\sum_i |I_i(hkl) - \langle I(hkl)\rangle|/\sum_{hkl}\sum_i I_i(hkl)$.

2.3. Data collection and processing

Drops containing the optimized crystals were overlaid with 2 µl mineral oil before the crystals were harvested and flash-cooled in liquid nitrogen. X-ray diffraction data were collected at 100 K from a single crystal on the ID30A-3 beamline of the European Synchrotron Radiation Facility (ESRF), Grenoble, France (Theveneau *et al.*, 2013). The data-collection strategy was calculated with *EDNA* (Incardona *et al.*, 2009) using four diffraction images at 0, 90, 180 and 270° with an oscillation

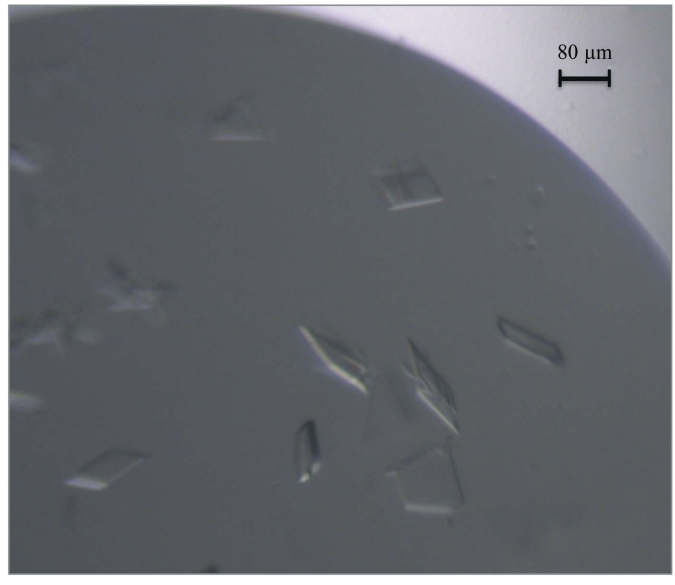

Figure 2
Crystals of NsrR. Rectangular plate-shaped crystals obtained using the sitting-drop vapour-diffusion method at 285 K.

width of 1° each. The subsequently collected data were processed and scaled using *XDS* and *XSCALE* (Kabsch, 2010*a*,*b*). Data-collection and processing statistics are summarized in Table 3.

3. Results and discussion

NsrR was successfully cloned and overexpressed in *E. coli* BL21 (DE3) cells. The protein was purified *via* a two-step purification protocol. Nickel-affinity chromatography was performed first, followed by size-exclusion chromatography (Fig. 1*a*). The yield of the protein was around 2 mg per litre of cell culture. Protein homogeneity and purity were assessed by SDS–PAGE (Fig. 1*b*). The molecular mass of the purified NsrR protein was comparable to the theoretically calculated molecular weight of 27.7 kDa (Gasteiger *et al.*, 2005).

Initial crystals of NsrR appeared after 2 d in PACT suite condition A5 [0.1 *M* SPG buffer pH 8.0, 25%(*w*/*v*) PEG 1500] using a sitting-drop setup. Optimizations were performed by varying the PEG concentration and the pH of the buffer. Rectangular plate-shaped crystals were obtained with 21–30%(*w*/*v*) PEG 1500, 0.1 *M* SPG buffer pH 8.0 after 1 d (Fig. 2), with maximum dimensions of 80 × 40 × 20 µm.

The rectangular plate-shaped crystals diffracted to 1.4 Å resolution using synchrotron X-rays (Fig. 3). The total data-collection time was 26 s. The crystals belonged to space group $P2_12_12$ (or its enantiomorph $P2_12_12_1$), with unit-cell parameters $a = 56.3$, $b = 60.4$, $c = 56.8$ Å, $\alpha = \beta = \gamma = 90°$ (Table 2). Currently, it is not possible to differentiate between space groups $P2_12_12$ or $P2_12_12_1$, as the systematic absences are not conclusive. The calculated Matthews coefficient resulted in a V_M of 1.75 Å^3 Da^{-1} and a solvent content of 29.6% for one monomer in the asymmetric unit (Matthews, 1968; Kantardjieff & Rupp, 2003). Mass-spectrometric analysis revealed 15 peptides covering 49% of the whole NsrR protein. Solving the structure by molecular replacement has so far failed, since all structures deposited in the PDB share a sequence identity at the amino-acid level of less than 34% (the BaeR structure has 33% identity; PDB entry 4b09; Choudhury & Beis, 2013), which therefore might not be sufficient. Reprocessing in space group *P*1 and subsequent molecular replacement also did not yield a satisfying solution. Hence, experimental phase determination is needed and we are currently attempting heavy-atom treatment using the optimized crystals.

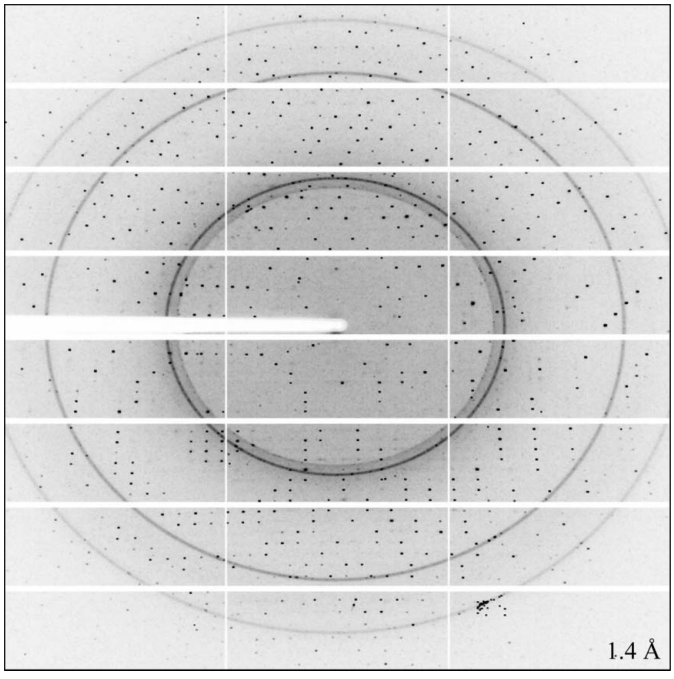

Figure 3
X-ray diffraction pattern of NsrR. Diffraction image of rectangular plate-shaped crystals of NsrR with an oscillation width of 1.0°. Four images at different angles were used to calculate the data-collection strategy using *EDNA* (Incardona *et al.*, 2009). The edge of the detector represents 1.4 Å.

NsrR represents a model for various two-component systems involved in lantibiotic resistance. The structure of NsrR would help us to further understand the mechanism of regulation behind lantibiotic resistance, thereby helping in its prevention.

Acknowledgements

The authors are grateful to Lutz Schmitt for his kind support, advice and invaluable suggestions. We would also like to thank André Abts for fruitful scientific discussions and Iris Fey for technical support. We acknowledge the European Synchrotron Radiation Facility for provision of synchrotron-radiation facilities and we would like to thank Philippe Carpentier for assistance in using beamline ID30A-3. We are also grateful to Heinrich-Heine International Graduate School of Protein Science and Technology (iGRASP$_{seed}$) for providing a scholarship to SK.

References

Bartoloni, A., Mantella, A., Goldstein, B., Dei, R., Benedetti, M., Sbaragli, S. & Paradisi, F. (2004). *J. Chemother.* **16**, 119–121.
Bergholz, T. M., Tang, S., Wiedmann, M. & Boor, K. J. (2013). *Appl. Environ. Microbiol.* **79**, 5682–5688.
Boakes, S. & Wadman, S. (2008). *Innov. Pharm. Technol.* **27**, 22–25.
Breukink, E. & de Kruijff, B. (2006). *Nature Rev. Drug Discov.* **5**, 321–323.
Choudhury, H. G. & Beis, K. (2013). *Protein Sci.* **22**, 1287–1293.
Cotter, P. D., Hill, C. & Ross, R. P. (2005). *Curr. Protein Pept. Sci.* **6**, 61–75.
Delves-Broughton, J., Blackburn, P., Evans, R. & Hugenholtz, J. (1996). *Antonie Van Leeuwenhoek*, **69**, 193–202.
Draper, L. A., Cotter, P. D., Hill, C. & Ross, R. P. (2015). *Microbiol. Mol. Biol. Rev.* **79**, 171–191.
Dyballa, N. & Metzger, S. (2009). *J. Vis. Exp.*, e1431.
Gasteiger, E., Hoogland, C., Gattiker, A., Wilkins, M. R., Appel, R. D. & Bairoch, A. (2005). *The Proteomics Protocols Handbook*, edited by J. M. Walker, pp. 571-607. Totowa: Humana Press.
Hancock, R. E. & Sahl, H.-G. (2006). *Nature Biotechnol.* **24**, 1551–1557.
Harris, L. J., Fleming, H. P. & Klaenhammer, T. R. (1992). *Food. Res. Int.* **25**, 57–66.
Hsu, S.-T. D., Breukink, E., Tischenko, E., Lutters, M. A. G., de Kruijff, B., Kaptein, R., Bonvin, A. M. J. J. & van Nuland, N. A. J. (2004). *Nature Struct. Mol. Biol.* **11**, 963–967.
Incardona, M.-F., Bourenkov, G. P., Levik, K., Pieritz, R. A., Popov, A. N. & Svensson, O. (2009). *J. Synchrotron Rad.* **16**, 872–879.

Kabsch, W. (2010*a*). *Acta Cryst.* D**66**, 125–132.
Kabsch, W. (2010*b*). *Acta Cryst.* D**66**, 133–144.
Kantardjieff, K. A. & Rupp, B. (2003). *Protein Sci.* **12**, 1865–1871.
Kawada-Matsuo, M., Oogai, Y., Zendo, T., Nagao, J., Shibata, Y., Yamashita, Y., Ogura, Y., Hayashi, T., Sonomoto, K. & Komatsuzawa, H. (2013). *Appl. Environ. Microbiol.* **79**, 4751–4755.
Kawada-Matsuo, M., Yoshida, Y., Zendo, T., Nagao, J., Oogai, Y., Nakamura, Y., Sonomoto, K., Nakamura, N. & Komatsuzawa, H. (2013). *PLoS One*, **8**, e69455.
Khosa, S., AlKhatib, Z. & Smits, S. H. J. (2013). *Biol. Chem.* **394**, 1543–1549.
Matthews, B. W. (1968). *J. Mol. Biol.* **33**, 491–497.
Severina, E., Severin, A. & Tomasz, A. (1998). *J. Antimicrob. Chemother.* **41**, 341–347.
Stock, A. M., Robinson, V. L. & Goudreau, P. N. (2000). *Annu. Rev. Biochem.* **69**, 183–215.
Suárez, J. M., Edwards, A. N. & McBride, S. M. (2013). *J. Bacteriol.* **195**, 2621–2631.
Theveneau, P. *et al.* (2013). *J. Phys. Conf. Ser.* **425**, 012001.